TU Delft

Delft University of Technology

Entropic uncertainty and measurement reversibility

Berta, Mario; Wehner, Stephanie; Wilde, Mark M.

DOI
10.1088/1367-2630/18/7/073004

Publication date
2016

Published in
New Journal of Physics

Citation (APA)
Berta, M., Wehner, S., & Wilde, M. M. (2016). Entropic uncertainty and measurement reversibility. *New Journal of Physics*, *18*, 1-13. https://doi.org/10.1088/1367-2630/18/7/073004

Important note
To cite this publication, please use the final published version (if applicable).
Please check the document version above.

Copyright
Other than for strictly personal use, it is not permitted to download, forward or distribute the text or part of it, without the consent of the author(s) and/or copyright holder(s), unless the work is under an open content license such as Creative Commons.

Takedown policy
Please contact us and provide details if you believe this document breaches copyrights.
We will remove access to the work immediately and investigate your claim.

This work is downloaded from Delft University of Technology.
For technical reasons the number of authors shown on this cover page is limited to a maximum of 10.

New Journal of Physics
The open access journal at the forefront of physics

Deutsche Physikalische Gesellschaft DPG IOP Institute of Physics

PAPER • OPEN ACCESS

Entropic uncertainty and measurement reversibility

To cite this article: Mario Berta *et al* 2016 *New J. Phys.* **18** 073004

View the article online for updates and enhancements.

Related content

- Measures and applications of quantum correlations
Gerardo Adesso, Thomas R Bromley and Marco Cianciaruso
- Optimal quantum networks and one-shot entropies
Giulio Chiribella and Daniel Ebler
- A channel-based framework for steering, non-locality and beyond
Matty J Hoban and Ana Belén Sainz

Recent citations

- Implementation of quantum secret sharing and quantum binary voting protocol in the IBM quantum computer
Dintomon Joy *et al*
- Exploration of entropic uncertainty relation for two accelerating atoms immersed in a bath of electromagnetic field
Zhiming Huang and Haozhen Situ
- Designing quantum router in IBM quantum computer
Bikash K. Behera *et al*

This content was downloaded from IP address 131.180.131.245 on 09/12/2019 at 08:44

New Journal of Physics
The open access journal at the forefront of physics

Deutsche Physikalische Gesellschaft DPG
IOP Institute of Physics

Published in partnership with: Deutsche Physikalische Gesellschaft and the Institute of Physics

OPEN ACCESS

RECEIVED
16 March 2016

REVISED
3 June 2016

ACCEPTED FOR PUBLICATION
20 June 2016

PUBLISHED
6 July 2016

Original content from this work may be used under the terms of the Creative Commons Attribution 3.0 licence.

Any further distribution of this work must maintain attribution to the author(s) and the title of the work, journal citation and DOI.

PAPER

Entropic uncertainty and measurement reversibility

Mario Berta[1], **Stephanie Wehner**[2] **and Mark M Wilde**[3,4]

[1] Institute for Quantum Information and Matter, California Institute of Technology, Pasadena, CA 91125, USA
[2] QuTech, Delft University of Technology, Lorentzweg 1, 2628 CJ Delft, The Netherlands
[3] Hearne Institute for Theoretical Physics, Department of Physics and Astronomy, Center for Computation and Technology, Louisiana State University, Baton Rouge, LA 70803, USA
[4] Author to whom any correspondence should be addressed.

E-mail: mwilde@lsu.edu

Keywords: uncertainty principle, quantum relative entropy, measurement reversibility

Abstract

The entropic uncertainty relation with quantum side information (EUR-QSI) from (Berta *et al* 2010 *Nat. Phys.* **6** 659) is a unifying principle relating two distinctive features of quantum mechanics: quantum uncertainty due to measurement incompatibility, and entanglement. In these relations, quantum uncertainty takes the form of preparation uncertainty where *one of two* incompatible measurements is applied. In particular, the 'uncertainty witness' lower bound in the EUR-QSI is not a function of a post-measurement state. An insightful proof of the EUR-QSI from (Coles *et al* 2012 *Phys. Rev. Lett.* **108** 210405) makes use of a fundamental mathematical consequence of the postulates of quantum mechanics known as the non-increase of quantum relative entropy under quantum channels. Here, we exploit this perspective to establish a tightening of the EUR-QSI which adds a new state-dependent term in the lower bound, related to how well one can reverse the action of a quantum measurement. As such, this new term is a direct function of the post-measurement state and can be thought of as quantifying how much disturbance a given measurement causes. Our result thus quantitatively unifies this feature of quantum mechanics with the others mentioned above. We have experimentally tested our theoretical predictions on the IBM *quantum experience* and find reasonable agreement between our predictions and experimental outcomes.

1. Introduction

The uncertainty principle is one of the cornerstones of modern physics, providing a striking separation between classical and quantum mechanics [1]. It is routinely used to reason about the behavior of quantum systems, and in recent years, an information-theoretic refinement of it that incorporates quantum side information has been helpful for witnessing entanglement and in establishing the security of quantum key distribution [2]. This latter refinement, known as the entropic uncertainty relation with quantum side information (EUR-QSI), is the culmination of a sequence of works spanning many decades [3–12] and is the one on which we focus here (see [13] for a survey).

Tripartite uncertainty relations. There are two variations of the EUR-QSI [2], one for tripartite and one for bipartite scenarios. Tripartite uncertainty relations capture an additional feature of quantum mechanics, namely the monogamy of entanglement [14]. Consider three systems, which we will refer to as Alice (A), Bob (B) and Eve (E). The monogamy of entanglement states that if A is very entangled with B, then A necessarily has very little entanglement with E. This physical effect is not only key to the security of quantum key distribution, but has far reaching consequences up to the recent firewall debate concerning the physics of black holes [15]. Tripartite uncertainty relations are one way to quantify the monogamy of entanglement by considering correlations amongst Alice, Bob and Eve. Let ρ_{ABE} denote a tripartite quantum state shared between Alice, Bob, and Eve, and let $\mathbb{X} \equiv \{P_A^x\}$ and $\mathbb{Z} = \{Q_A^z\}$ be projection-valued measures (PVMs) that can be performed on Alice's system (note that considering PVMs implies statements for the more general positive operator-valued measures, by invoking the Naimark extension theorem [16]). If Alice chooses to measure $\mathbb{X}$, then the post-measurement state

© 2016 IOP Publishing Ltd and Deutsche Physikalische Gesellschaft

is as follows:

$$\sigma_{XBE} \equiv \sum_x |x\rangle\langle x|_X \otimes \sigma^x_{BE}, \qquad \text{where}$$
$$\sigma^x_{BE} \equiv \mathrm{Tr}_A\{(P^x_A \otimes I_{BE})\rho_{ABE}\}. \tag{1}$$

Similarly, if Alice instead chooses to measure $\mathbb{Z}$, then the post-measurement state is

$$\omega_{ZBE} \equiv \sum_z |z\rangle\langle z|_Z \otimes \omega^z_{BE}, \qquad \text{where}$$
$$\omega^z_{BE} \equiv \mathrm{Tr}_A\{(Q^z_A \otimes I_{BE})\rho_{ABE}\}. \tag{2}$$

In the above, $\{|x\rangle_X\}_x$ and $\{|z\rangle_Z\}_z$ are orthonormal bases that encode the classical outcome of the respective measurements. The following tripartite EUR-QSI in (3) quantifies the trade-off between Bob's ability to predict the outcome of the $\mathbb{X}$ measurement with the help of his quantum system B and Eve's ability to predict the outcome of the $\mathbb{Z}$ measurement with the help of her system E:

$$H(X|B)_\sigma + H(Z|E)_\omega \geqslant -\log c, \tag{3}$$

where here and throughout we take the logarithm to have base two. In the above

$$H(F|G)_\tau \equiv H(FG)_\tau - H(G)_\tau = H(\tau_{FG}) - H(\tau_G) \tag{4}$$

denotes the conditional von Neumann entropy of a state τ_{FG}, with $H(\tau) \equiv -\mathrm{Tr}\{\tau \log \tau\}$, and the parameter c captures the incompatibility of the $\mathbb{X}$ and $\mathbb{Z}$ measurements:

$$c \equiv \max_{x,z} \|P^x_A Q^z_A\|^2_\infty \in [0,\ 1]. \tag{5}$$

The conditional entropy $H(F|G)_\tau$ is a measure of the uncertainty about system F from the perspective of someone who possesses system G, given that the state of both systems is τ_{FG}. The uncertainty relation in (3) thus says that if Bob can easily predict X given B (i.e., $H(X|B)$ is small) and the measurements are incompatible, then it is difficult for Eve to predict Z given E (i.e., $H(Z|E)$ is large). As such, (5) at the same time quantifies measurement incompatibility and the monogamy of entanglement [17]. A variant of (3) in terms of the conditional min-entropy [18] can be used to establish the security of quantum key distribution under particular assumptions [19, 20].

The EUR-QSI in (3) can be summarized informally as a game involving a few steps. To begin with, Alice, Bob, and Eve are given a state ρ_{ABE}. Alice then flips a coin to decide whether to measure $\mathbb{X}$ or $\mathbb{Z}$. If she gets heads, she measures $\mathbb{X}$ and tells Bob that she did so. Bob then has to predict the outcome of her $\mathbb{X}$ measurement and can use his quantum system B to help do so. If Alice gets tails, she instead measures $\mathbb{Z}$ and tells Eve that she did so. In this case, Eve has to predict the outcome of Alice's $\mathbb{Z}$ measurement and can use her quantum system E as an aid. There is a trade-off between their ability to predict correctly, which is captured by (3).

Bipartite uncertainty relations. We now recall the second variant of the EUR-QSI from [2]. Such bipartite relations can be used to quantify and witness aspects of entanglement shared between only two parties, Alice and Bob. Here we have a bipartite state ρ_{AB} shared between Alice and Bob and again the measurements $\mathbb{X}$ and $\mathbb{Z}$ mentioned above. Alice chooses to measure either $\mathbb{X}$ or $\mathbb{Z}$, leading to the respective post-measurement states σ_{XB} and ω_{ZB} defined from (1) and (2) after taking a partial trace over the E system. The following EUR-QSI in (6) quantifies the trade-off between Bob's ability to predict the outcome of the $\mathbb{X}$ or $\mathbb{Z}$ measurement:

$$H(Z|B)_\omega + H(X|B)_\sigma \geqslant -\log c + H(A|B)_\rho, \tag{6}$$

where the incompatibility parameter c is defined in (5) and the conditional entropy $H(A|B)_\rho$ is a signature of both the mixedness and entanglement of the state ρ_{AB}. For (6) to hold, we require the technical condition that the $\mathbb{Z}$ measurement be a rank-one measurement [21] (however see also [22, 23] for a lifting of this condition). The EUR-QSI in (6) finds application in witnessing entanglement, as discussed in [2].

The uncertainty relation in (6) can also be summarized informally as a game, similar to the one discussed above. Here, we have Alice choose whether to measure $\mathbb{X}$ or $\mathbb{Z}$. If she measures $\mathbb{X}$, she informs Bob that she did so, and it is his task to predict the outcome of the $\mathbb{X}$ measurement. If she instead measures $\mathbb{Z}$, she tells Bob, and he should predict the outcome of the $\mathbb{Z}$ measurement. In both cases, Bob is allowed to use his quantum system B to help in predicting the outcome of Alice's measurement. Again there is generally a trade-off between how well Bob can predict the outcome of the $\mathbb{X}$ or $\mathbb{Z}$ measurement, which is quantified by (6). The better that Bob can predict the outcome of either measurement, the more entangled the state ρ_{AB} is.

2. Main result

The main contribution of the present paper is to refine and tighten both of the uncertainty relations in (3) and (6) by employing a recent result from [24] (see also [25–27]). This refinement adds a term involving measurement

reversibility, next to the original trade-offs in terms of measurement incompatibility and entanglement. An insightful proof of the EUR-QSIs above makes use of an entropy inequality known as the non-increase of quantum relative entropy [28, 29]. This entropy inequality is fundamental in quantum physics, providing limitations on communication protocols [30] and thermodynamic processes [31]. The main result of [24–27] offers a strengthening of the non-increase of quantum relative entropy, quantifying how well one can recover from the deleterious effects of a noisy quantum channel. Here we apply the particular result from [24] to establish a tightening of both uncertainty relations in (3) and (6) with a term related to how well one can 'reverse' an additional $\mathbb{X}$ measurement performed on Alice's system at the end of the uncertainty game, if the outcome of the $\mathbb{X}$ measurement and the B system are available. The upshot is an entropic uncertainty relation which incorporates measurement reversibility in addition to quantum uncertainty due to measurement incompatibility, and entanglement, thus unifying several genuinely quantum features into a single uncertainty relation.

In particular, we establish the following refinements of (3) and (6):

$$H(Z|E)_\omega + H(X|B)_\sigma \geqslant -\log c - \log f, \tag{7}$$

$$H(Z|B)_\omega + H(X|B)_\sigma \geqslant -\log c - \log f + H(A|B)_\rho, \tag{8}$$

where c is defined in (5),

$$f \equiv F(\rho_{AB}, \mathcal{R}_{XB\to AB}(\sigma_{XB})), \tag{9}$$

and in (8) we need the projective $\mathbb{Z}$ measurement to be a rank-one measurement (i.e., $Q_A^z = |z\rangle\langle z|$). In addition to the measurement incompatibility c, the term f quantifies the disturbance caused by one of the measurements, in particular, how reversible such a measurement is. $F(\rho_1, \rho_2) \equiv \|\sqrt{\rho_1}\sqrt{\rho_2}\|_1^2$ denotes the quantum fidelity between two density operators ρ_1 and ρ_2 [32], and $\mathcal{R}_{XB\to AB}$ is a *recovery* quantum channel with input systems XB and output systems AB. Appendix A details a proof for (7) and (8). In section 4, we discuss several simple exemplary states and measurements to which (8) applies, and in section 5, we detail the results of several experimental tests of the theoretical predictions, finding reasonable agreement between the experimental results and our predictions.

In the case that the $\mathbb{Z}$ measurement has the form $\{Q_A^z = |z\rangle\langle z|_A\}_z$ for an orthonormal basis $\{|z\rangle_A\}_z$, the action of the recovery quantum channel $\mathcal{R}_{XB\to AB}$ on an arbitrary state ξ_{XB} is explicitly given as follows (see appendix B for details):

$$\mathcal{R}_{XB\to AB}(\xi_{XB}) = \sum_{z,x,z'} |z\rangle\langle z|_A P_A^x |z'\rangle\langle z'|_A \otimes \mathcal{R}_{XB\to B}^{x,z,z'}(\xi_{XB}), \tag{10}$$

where

$$\mathcal{R}_{XB\to B}^{x,z,z'}(\xi_{XB}) \equiv \int_{-\infty}^{\infty} \mathrm{d}t\ p(t)(\omega_B^z)^{\frac{1-it}{2}}(\theta_B^x)^{\frac{-1+it}{2}}\mathrm{Tr}_X\{|x\rangle\langle x|_X(\xi_{XB})\}(\theta_B^x)^{\frac{-1-it}{2}}(\omega_B^{z'})^{\frac{1+it}{2}}, \tag{11}$$

with the probability density $p(t) \equiv \frac{\pi}{2}(\cosh(\pi t) + 1)^{-1}$. (Note that $\mathcal{R}_{XB\to B}^{x,z,z'}$ is not a channel—we are merely using this notation as a shorthand.) In the above, θ_{XB} is the state resulting from Alice performing the $\mathbb{Z}$ measurement, following with the $\mathbb{X}$ measurement, and then discarding the outcome of the $\mathbb{Z}$ measurement:

$$\theta_{XB} \equiv \sum_x |x\rangle\langle x|_X \otimes \theta_B^x \quad \text{with}$$
$$\theta_B^x \equiv \sum_z \langle z|P_A^x|z\rangle\,\omega_B^z. \tag{12}$$

For this case, ω_B^z from (2) reduces to $\omega_B^z = (\langle z|_A \otimes I_B)\rho_{AB}(|z\rangle_A \otimes I_B)$. As one can readily check by plugging into (10), the recovery channel $\mathcal{R}$ has the property that it perfectly reverses an $\mathbb{X}$ measurement if it is performed after a $\mathbb{Z}$ measurement:

$$\mathcal{R}_{XB\to AB}(\theta_{XB}) = \sum_z |z\rangle\langle z|_A \otimes \omega_B^z. \tag{13}$$

The fidelity $F(\rho_{AB}, \mathcal{R}_{XB\to AB}(\sigma_{XB}))$ thus quantifies how much disturbance the $\mathbb{X}$ measurement causes to the original state ρ_{AB} in terms of how well the recovery channel $\mathcal{R}$ can reverse the process. We note that there is a trade-off between reversing the $\mathbb{X}$ measurement whenever it is greatly disturbing ρ_{AB} and meeting the constraint in (13). Since the quantum fidelity always takes a value between zero and one, it is clear that (7) and (8) represent a state-dependent tightening of (3) and (6), respectively.

3. Interpretation

It is interesting to note that just as the original relation in (6) could be used to witness entanglement, the new relation can be used to witness both entanglement and recovery from measurement, as will be illustrated using

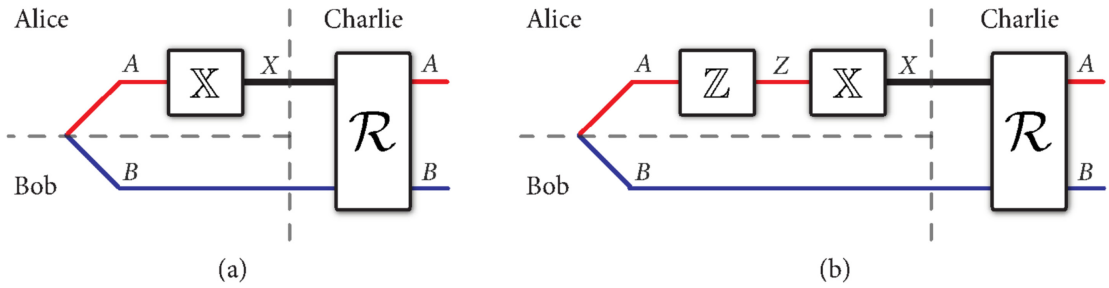

Figure 1. Measurement reversibility game. How well can Charlie reverse the action of the $\mathbb{X}$ measurement in either scenario (a) or (b)? The quantities in (7) and (8) other than f constitute a 'recoverability witness,' quantifying Charlie's ability to do so.

the examples below. That is, having low conditional entropy for both measurement outcomes constitutes a recoverability witness, when given information about the entanglement.

We recalled above the established 'uncertainty games' in order to build an intuition for (3) and (6). In order to further understand the refinements in (7) and (8), we could imagine that after either game is completed, we involve another player Charlie. Regardless of which measurement Alice performed in the original game, she then performs an additional $\mathbb{X}$ measurement. Bob sends his quantum system B to Charlie, and Alice sends the classical outcome of the final $\mathbb{X}$ measurement to Charlie. It is then Charlie's goal to 'reverse' the $\mathbb{X}$ measurement in either of the scenarios above, and his ability to do so is limited by the uncertainty relations in (7) and (8). Figure 1 depicts this game. In the case that (a) Alice performed an $\mathbb{X}$ measurement in the original game, the state that Charlie has is σ_{XB}. In the case that (b) Alice performed a $\mathbb{Z}$ measurement in the original game, then the state that Charlie has is θ_{XB}. Not knowing which state he has received, Charlie can perform the recovery channel $\mathcal{R}$ and be guaranteed to restore the state to

$$\sum_z |z\rangle\langle z| \otimes (\langle z| \otimes I_B)\rho_{AB}(|z\rangle \otimes I_B) \tag{14}$$

in the case that (b) occurred, while having a performance limited by (7) or (8) in the case that (a) occurred.

4. Examples

It is helpful to examine some examples in order to build an intuition for our refinements of the EUR-QSIs. Here we focus on the bipartite EUR-QSI in (8) and begin by evaluating it for some 'minimum uncertainty states' [21] (see also [33]). These are states for which the original uncertainty relation in (6) is already tight, i.e., an equality. Later, we will consider the case of a representative 'maximum uncertainty state,' that is, a state for which the original uncertainty relation (6) is maximally non-tight. This last example distinguishes our new contribution in (8) from the previously established bound in (6).

For all of the forthcoming examples, we take the $\mathbb{X}$ measurement to be Pauli σ_X and the $\mathbb{Z}$ measurement to be Pauli σ_Z, which implies that $-\log c = 1$. We define the 'BB84' states $|0\rangle$, $|1\rangle$, $|+\rangle$, and $|-\rangle$ from the following relations:

$$\sigma_Z|0\rangle = |0\rangle, \qquad \sigma_Z|1\rangle = (-1)|1\rangle, \qquad \sigma_X|+\rangle = |+\rangle, \qquad \sigma_X|-\rangle = (-1)|-\rangle. \tag{15}$$

So this means that the $\mathbb{X}$ and $\mathbb{Z}$ measurements have the following respective implementations as quantum channels acting on an input ξ:

$$\xi \to \langle +|_A \xi |+\rangle_A |0\rangle\langle 0|_X + \langle -|_A \xi |-\rangle_A |1\rangle\langle 1|_X, \tag{16}$$

$$\xi \to \langle 0|_A \xi |0\rangle_A |0\rangle\langle 0|_Z + \langle 1|_A \xi |1\rangle_A |1\rangle\langle 1|_Z. \tag{17}$$

4.1. Minimum uncertainty states

4.1.1. X eigenstate on system A

First suppose that $\rho_{AB} = |+\rangle\langle +|_A \otimes \pi_B$, where π is the maximally mixed state. In this case, Bob's system B is of no use to help predict the outcome of a measurement on the A system because the systems are in a product state. Here we find by direct calculation that $H(A|B)_\rho = 0$, $H(X|B)_\sigma = 0$, and $H(Z|B)_\omega = 1$. By (8), this then implies that there exists a recovery channel $\mathcal{R}^{(1)}$ such that (13) is satisfied and, given that $\sigma_{XB} = |0\rangle\langle 0|_X \otimes \pi_B$, we also have the perfect recovery

$$\mathcal{R}^{(1)}_{XB\to AB}(|0\rangle\langle 0|_X \otimes \pi_B) = |+\rangle\langle +|_A \otimes \pi_B. \tag{18}$$

To determine the recovery channel $\mathcal{R}^{(1)}$, consider that

$$\sum_z |z\rangle\langle z|_Z \otimes \omega^z_B = \pi_Z \otimes \pi_B, \qquad \sum_x |x\rangle\langle x|_X \otimes \theta^x_B = \pi_X \otimes \pi_B, \tag{19}$$

with the states on the left in each case defined in (2) and (12), respectively. Plugging into (10), we find that the recovery channel in this case is given explicitly by

$$\mathcal{R}^{(1)}_{XB\to AB}(\xi_{XB}) = |+\rangle\langle +|_A \otimes \mathrm{Tr}_X\{|0\rangle\langle 0|_X \xi_{XB}\} + |-\rangle\langle -|_A \otimes \mathrm{Tr}_X\{|1\rangle\langle 1|_X \xi_{XB}\}, \tag{20}$$

so that we also see that

$$\mathcal{R}^{(1)}_{XB\to AB}(\pi_X \otimes \pi_B) = \pi_A \otimes \pi_B. \tag{21}$$

4.1.2. Z eigenstate on system A

The situation in which $\rho_{AB} = |0\rangle\langle 0|_A \otimes \pi_B$ is similar in some regards, but the recovery channel is different—i.e., we have by direct calculation that $H(A|B)_\rho = 0$, $H(X|B)_\sigma = 1$, and $H(Z|B)_\omega = 0$, which implies the existence of a different recovery channel $\mathcal{R}^{(2)}$ such that (13) is satisfied, and given that $\sigma_{XB} = \pi_X \otimes \pi_B$, we also have the perfect recovery

$$\mathcal{R}^{(2)}_{XB\to AB}(\pi_X \otimes \pi_B) = |0\rangle\langle 0|_A \otimes \pi_B. \tag{22}$$

To determine the recovery channel $\mathcal{R}^{(2)}$, consider that

$$\sum_z |z\rangle\langle z|_Z \otimes \omega^z_B = |0\rangle\langle 0|_Z \otimes \pi_B, \qquad \sum_x |x\rangle\langle x|_X \otimes \theta^x_B = \pi_X \otimes \pi_B, \tag{23}$$

with the states on the left in each case defined in (2) and (12), respectively. Plugging into (10), we find that the recovery channel in this case is given explicitly by

$$\mathcal{R}^{(2)}_{XB\to AB}(\xi_{XB}) = |0\rangle\langle 0|_A \otimes \mathrm{Tr}_X\{\xi_{XB}\}. \tag{24}$$

4.1.3. Maximally entangled state on systems A and B

Now suppose that $\rho_{AB} = |\Phi\rangle\langle\Phi|_{AB}$ is the maximally entangled state, where $|\Phi\rangle_{AB} \equiv (|00\rangle_{AB} + |11\rangle_{AB})/\sqrt{2}$. In this case, we have that both $H(X|B)_\sigma = 0$ and $H(Z|B)_\omega = 0$, but the conditional entropy is negative: $H(A|B)_\rho = -1$. So here again we find the existence of a recovery channel $\mathcal{R}^{(3)}$ such that (13) is satisfied, and given that $\sigma_{XB} = (|0+\rangle\langle 0+|_{XB} + |1-\rangle\langle 1-|_{XB})/2$, we also have the perfect recovery

$$\mathcal{R}^{(3)}_{XB\to AB}((|0+\rangle\langle 0+|_{XB} + |1-\rangle\langle 1-|_{XB})/2) = |\Phi\rangle\langle\Phi|_{AB}. \tag{25}$$

To determine the recovery channel $\mathcal{R}^{(3)}$, consider that

$$\sum_z |z\rangle\langle z|_Z \otimes \omega^z_B = \frac{1}{2}(|0\rangle\langle 0|_Z \otimes |0\rangle\langle 0|_B + |1\rangle\langle 1|_Z \otimes |1\rangle\langle 1|_B), \tag{26}$$

$$\sum_x |x\rangle\langle x|_X \otimes \theta^x_B = \pi_X \otimes \pi_B, \tag{27}$$

with the states on the left in each case defined in (2) and (12), respectively. Plugging into (10), we find that the recovery channel in this case is given explicitly by

$$\mathcal{R}^{(3)}_{XB\to AB}(\xi_{XB}) = \sum_{z,z',x\in\{0,1\}} (-1)^{x(z+z')} |z\rangle\langle z'|_A \otimes |z\rangle\langle z'|_B \mathrm{Tr}\{|x\rangle\langle x|_X \otimes |z'\rangle\langle z|_B \xi_{XB}\}, \tag{28}$$

i.e., with the following Kraus operators:

$$\left\{\sum_z (-1)^{xz} (|z\rangle_A \otimes |z\rangle_B)(\langle x|_X \otimes \langle z|_B)\right\}_x. \tag{29}$$

These Kraus operators give the recovery map $\mathcal{R}^{(3)}_{XB\to AB}$ the interpretation of (1) measuring the X register and (2) coherently copying the contents of the B register to the A register along with an appropriate relative phase. It can be implemented by performing a controlled-NOT gate from B to A, followed by a controlled-phase gate on X and B and a partial trace over system X.

Remark 1. All of the examples mentioned above involve a perfect recovery or a perfect reversal of the $\mathbb{X}$ measurement. This is due to the fact that the bound in (6) is saturated for these examples. However, the refined inequality in (8) allows to generalize these situations to the approximate case, in which ρ_{AB} is nearly indistinguishable from the states given above. It is then the case that the equalities in (18)–(25) become approximate equalities, with a precise characterization given by (8).

4.2. Maximum uncertainty states

We now investigate the extreme opposite situation, when the bound in (6) is far from being saturated but its refinement in (8) is saturated. Let $\rho_{AB} = |+_Y\rangle\langle+_Y|_A \otimes \pi_B$, where $|+_Y\rangle$ is defined from the relation $\sigma_Y|+_Y\rangle = |+_Y\rangle$. In this case, we find that both $H(X|B)_\sigma = 1$ and $H(Z|B)_\omega = 1$. Thus, we could say that ρ_{AB} is a 'maximum uncertainty state' because the sum $H(X|B)_\sigma + H(Z|B)_\omega$ is equal to two bits and cannot be any larger than this amount. We also find that $H(A|B)_\rho = 0$, implying that (6) is one bit away from being saturated. Now consider that $\sigma_{XB} = \theta_{XB} = \pi_X \otimes \pi_B$ and $\omega_{ZB} = \pi_Z \otimes \pi_B$, and thus one can explicitly calculate the recovery channel $\mathcal{R}^{(4)}$ from (10) to take the form:

$$\mathcal{R}^{(4)}_{XB\to AB}(\xi_{XB}) \equiv |+\rangle\langle+|_A \otimes \mathrm{Tr}_X\{|0\rangle\langle 0|_X \xi_{XB}\} + |-\rangle\langle-|_A \otimes \mathrm{Tr}_X\{|1\rangle\langle 1|_X \xi_{XB}\}. \tag{30}$$

Note that the recovery channel $\mathcal{R}^{(4)}_{XB\to AB}$ is the same as $\mathcal{R}^{(1)}_{XB\to AB}$ in (20).

This implies that

$$\mathcal{R}^{(4)}_{XB\to AB}(\sigma_{XB}) = \pi_A \otimes \pi_B, \tag{31}$$

$$\mathcal{R}^{(4)}_{XB\to AB}(\theta_{XB}) = \pi_A \otimes \pi_B, \tag{32}$$

and in turn that

$$-\log F(\rho_{AB}, \mathcal{R}^{(4)}_{XB\to AB}(\theta_{XB})) = 1. \tag{33}$$

Thus the inequality in (8) is saturated for this example. The key element is that there is one bit of uncertainty when measuring a Y eigenstate with respect to either the X or Z basis. At the same time, the Y eigenstate is pure, so that its entropy is zero. This leaves a bit of uncertainty available and for which (6) does not account, but which we have now interpreted in terms of how well one can reverse the $\mathbb{X}$ measurement, using the refined bound in (8). One could imagine generalizing the idea of this example to higher dimensions in order to find more maximum uncertainty examples of this sort.

5. Experiments

We have experimentally tested three of the examples from the previous section, namely, the X eigenstate, the maximally entangled state, and the Y eigenstate examples. We did so using the recently available IBM *quantum experience* (QE) [34]. Three experiments have already appeared on the arXiv, conducted remotely by theoretical groups testing out experiments which had never been performed previously [35–37]. The QE architecture consists of five fixed-frequency superconducting transmon qubits, laid out in a 'star geometry' (four 'corner' qubits and one in the center). It is possible to perform single-qubit gates X, Y, Z, H, T, S, and $S^\dagger$, a Pauli measurement Z, and Bloch sphere tomography on any single qubit. However, two-qubit operations are limited to controlled-NOT gates with any one of the corner qubits acting as the source and the center qubit as the target. Thus, one must 'recompile' quantum circuits in order to meet these constraints. More information about the architecture is available at the user guide at [34].

Our experiments realize and test three of the examples from the previous section and, in particular, are as follows:

(1) Prepare system A in the state $|+\rangle$. Measure Pauli σ_X on qubit A and place the outcome in register X. Perform the recovery channel given in (20), with output system A'. Finally, perform Bloch sphere tomography on system A'.

(2) Prepare system A in the state $|+\rangle$. Measure Pauli σ_Z on qubit A and place the outcome in register Z. Measure Pauli σ_X on qubit A and place the outcome in register X. Perform the recovery channel given in (20), with output system A'. Finally, perform Bloch sphere tomography on system A'.

(3) Same as Experiment 1 but begin by preparing system A in the state $|+_Y\rangle_A$.

(4) Same as Experiment 2 but begin by preparing system A in the state $|+_Y\rangle_A$.

(5) Prepare systems A and B in the maximally entangled Bell state $|\Phi\rangle_{AB}$. Measure Pauli σ_X on qubit A and place the outcome in register X. Perform the recovery channel given in (28), with output systems A' and B. Finally, perform measurements of σ_X on system A' and σ_X on system B, or σ_Y on system A' and σ_Y^* on system B, or σ_Z on system A' and σ_Z on system B.

(6) Prepare systems A and B in the maximally entangled Bell state $|\Phi\rangle_{AB}$. Measure Pauli σ_Z on qubit A and place the outcome in register Z. Measure Pauli σ_X on qubit A and place the outcome in register X. Perform the recovery channel given in (28), with output systems A' and B. Finally, perform measurements of σ_X on

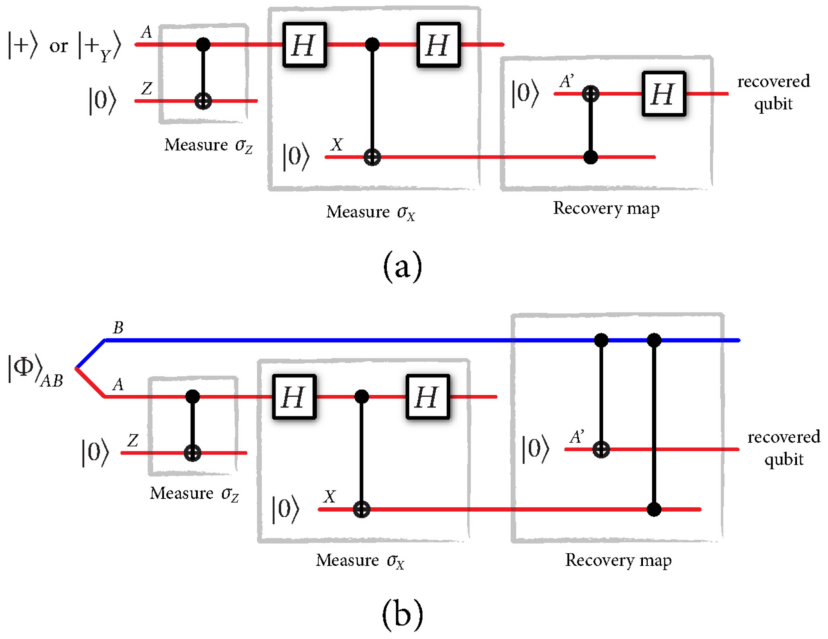

Figure 2. Circuits for testing our entropic uncertainty relation in (8) experimentally. (a) Four different experimental tests in which one can prepare system A as either $|+\rangle_A$ or $|+_Y\rangle_A$ and then perform either a σ_Z Pauli measurement or not. This measurement is implemented by transferring the information in the σ_Z basis to an environment Z (box 1 labeled 'measure σ_Z'). Measuring the Z qubit in the standard basis provides the measurement result. Afterwards, a σ_X measurement is performed followed by the recovery operation from (20), whose aim it is to undo the effect of the σ_X measurement. If $|+\rangle_A$ is prepared and σ_Z is not measured (box 1 is not included), then it is possible to undo the effect of the σ_X measurement and recover the qubit $|+\rangle$ perfectly in system A'. If $|+\rangle_A$ is prepared and σ_Z is then measured (box 1 is included), it is possible to undo the effect of the σ_X measurement with the same recovery operation. The same results hold if $|+_Y\rangle_A$ is prepared in system A (i.e., the recovery operation undoes the effect of the σ_X measurement). (b) Two different experimental tests in which one can prepare a maximally entangled Bell state $|\Phi\rangle_{AB}$ in systems A and B, perform a Pauli σ_Z measurement or not (i.e., box 1 is either included or not), perform a σ_X measurement, followed by a recovery operation whose aim it is to undo the effect of the σ_X measurement. In the case that σ_Z is not measured, the recovery operation perfectly restores the maximally entangled state in systems A' and B. In the case that σ_Z is measured, the recovery operation undoes the effect of the σ_X measurement by restoring the maximally correlated state $(|00\rangle\langle 00|_{A'B} + |11\rangle\langle 11|_{A'B})/2$ in systems A' and B.

system A' and σ_X on system B, or σ_Y on system A' and σ_Y^* on system B, or σ_Z on system A' and σ_Z on system B.

A quantum circuit that can realize Experiments 1–4 is given in figure 2(a), and a quantum circuit that can realize Experiments 5–6 is given in figure 2 (b). These circuits make use of standard quantum computing gates, detailed in [38], and one can readily verify that they ideally have the correct behavior, consistent with that discussed for the examples in the previous section. As stated above, it is necessary to recompile these circuits into a form which meets the constraints of the QE architecture.

Figure 3 plots the results of Experiments 1–6. Each experiment consists of three measurements, with Experiments 1–4 having measurements of each of the Pauli operators, and Experiments 5–6 having three different measurements each as outlined above. Each of these is repeated 8192 times, for a total of $6 \times 3 \times 8192 = 147,456$ experiments. The standard error for each kind of experiment is thus $\sqrt{p_c(1-p_c)/8192}$, where p_c is the estimate of the probability of a given measurement outcome in a given experiment. The caption of figure 3 features discussions of and comparisons between the predictions of the previous section and the experimental outcomes. While it is clear that the QE chip is subject to significant noise, there is still reasonable agreement with the theoretical predictions of the previous section. One observation we make regarding figure 3(e) is that the frequencies for the outcomes of the σ_Z and σ_Z measurements are much closer to the theoretically predicted values than are the other measurement outcomes.

6. Conclusion

The EUR-QSI is a unifying principle relating quantum uncertainty due to measurement incompatibility and entanglement. Here we refine and tighten this inequality with a state-dependent term related to how well one can reverse the action of a measurement. The tightening of the inequality is most pronounced when the measurements and state are all chosen from mutually unbiased bases, i.e., in our 'maximum uncertainty' example with the measurements being σ_X and σ_Z and the initial state being a σ_Y eigenstate. We have

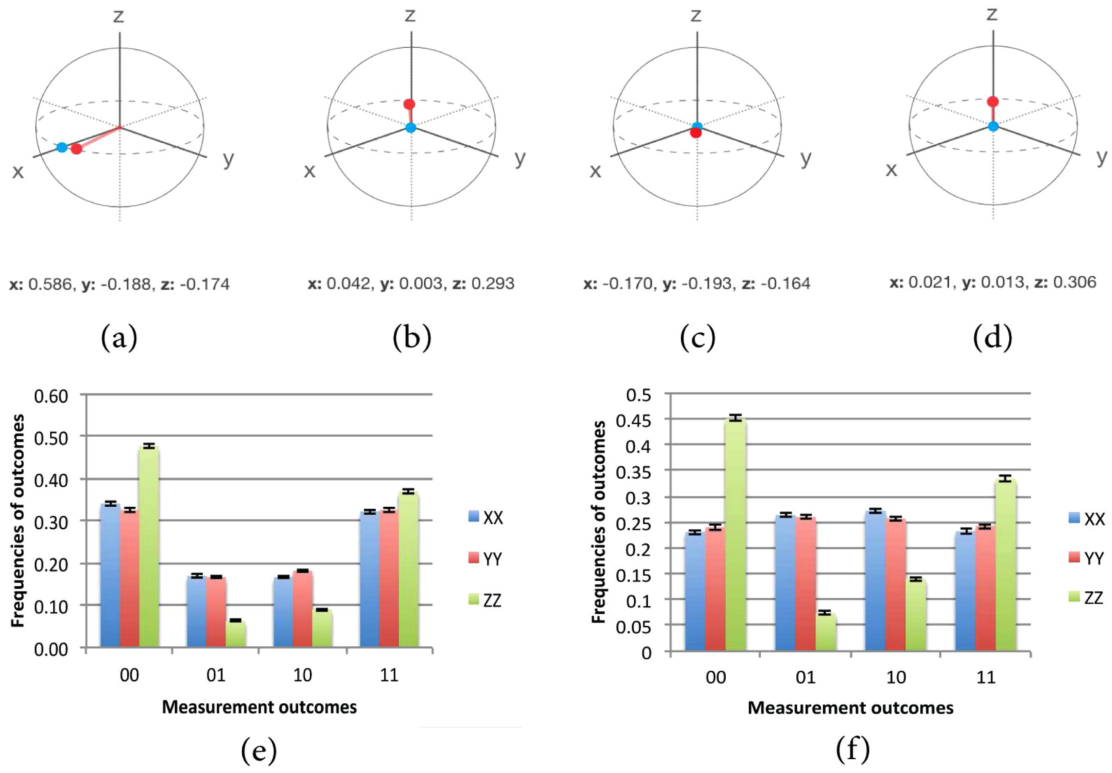

Figure 3. Results of experimental tests on the IBM QE quantum computer. Subfigures (a)–(f) correspond to Experiments 1–6 outlined in the main text, respectively. (a) The ideal state of the recovered qubit is $|+\rangle$, as predicted by (18) and depicted on the Bloch sphere as a blue dot. The figure plots the result of Bloch sphere tomography from the experimental tests (as a red dot, figures taken from the IBM QE site). (b)–(d) The ideal state of the recovered qubit in each case is π (the maximally mixed state), as predicted by (21), (31), and (32), respectively (again depicted as blue dots). The figure again plots the result of Bloch sphere tomography as red dots. (e) The ideal state of the recovered qubits is $|\Phi\rangle$ as predicted by (25). In such a case, measurement of the Pauli observables σ_i on A' and σ_i^* on B for $i \in \{X, Y, Z\}$ should return 00 and 11 with probability 0.5 and 01 and 10 with probability zero. The plots reveal significant noise in the experiments, especially from the σ_X and σ_Y measurements. (f) The ideal state of the recovered qubits is the maximally correlated state $(|00\rangle\langle 00| + |11\rangle\langle 11|)/2$ as predicted in section 4.1.3. In such a case, measurement of the Pauli observables σ_Z on A and σ_Z on B should return 00 and 11 with probability 0.5 and 01 and 10 with probability zero. Measurement of the Pauli observables σ_i on A and σ_i^* on B for $i \in \{X, Y\}$ should return all outcomes with equal probabilities. Again, the plots reveal significant noise in the experiments.

experimentally tested our theoretical predictions on the IBM QE and find reasonable agreement between our predictions and experimental outcomes.

We note that in terms of the conditional min-entropy, other refinements of (6) are known [39] that look at the measurement channel and its own inverse channel, and it would be interesting to understand their relation. Going forward, it would furthermore be interesting to generalize the results established here to infinite-dimensional and multiple measurement scenarios.

Acknowledgments

The authors acknowledge discussions with Siddhartha Das, Michael Walter, and Andreas Winter. We are grateful to the team at IBM and the IBM Quantum Experience project. This work does not reflect the views or opinions of IBM or any of its employees. MB acknowledges funding provided by the Institute for Quantum Information and Matter, an NSF Physics Frontiers Center (NSF Grant PHY-1125565) with support of the Gordon and Betty Moore Foundation (GBMF-12500028). Additional funding support was provided by the ARO grant for Research on Quantum algorithms at the IQIM (W911NF-12-1-0521). SW acknowledges support from STW, Netherlands and an NWO VIDI Grant. MMW is grateful to SW and her group for hospitality during a research visit to QuTech in May 2015 and acknowledges support from startup funds from the Department of Physics and Astronomy at LSU, the NSF under Award No. CCF-1350397, and the DARPA Quiness Program through US Army Research Office award W31P4Q-12-1-0019.

Appendix A. Proof of (7) and (8)

The main idea of the proof of (7) follows the approach first put forward in [21] (see also [33]), for which the core argument is the non-increase of quantum relative entropy. Here we instead apply a refinement of this entropy inequality from [24] (see also [25–27]). In order to prove (7), we start by noting that it suffices to prove it when $\rho_{ABE} = |\psi\rangle\langle\psi|_{ABE}$ (i.e., the shared state is pure). This is because the conditional entropy only increases under the discarding of one part of the conditioning system. We consider the following isometric extensions of the measurement channels [40], which produce the measurement outcomes and post-measurement states:

$$U_{A\to XX'A} \equiv \sum_x |x\rangle_X \otimes |x\rangle_{X'} \otimes P_A^x, \tag{A1}$$

$$V_{A\to ZZ'A} \equiv \sum_z |z\rangle_Z \otimes |z\rangle_{Z'} \otimes Q_A^z. \tag{A2}$$

We also define the following pure states, which represent purifications of the states σ_{XBE} and ω_{ZBE} defined in (1) and (2), respectively:

$$|\sigma\rangle_{XX'ABE} \equiv U_{A\to XX'A}|\psi\rangle_{ABE}, \tag{A3}$$

$$|\omega\rangle_{ZZ'ABE} \equiv V_{A\to ZZ'A}|\psi\rangle_{ABE}. \tag{A4}$$

Consider from duality of conditional entropy for pure states (see, e.g., [33]) that

$$H(Z|E)_\omega = -H(Z|Z'AB)_\omega = D(\omega_{ZZ'AB}\|I_Z \otimes \omega_{Z'AB}), \tag{A5}$$

where $D(\rho\|\sigma) \equiv \mathrm{Tr}\{\rho[\log\rho - \log\sigma]\}$ is the quantum relative entropy [41], defined as such when $\mathrm{supp}(\rho) \subseteq \mathrm{supp}(\sigma)$ and as $+\infty$ otherwise. Now consider the following quantum channel

$$\mathcal{P}_{ZZ'A}(\cdot) \to \Pi(\cdot)\Pi + (I-\Pi)(\cdot)(I-\Pi), \tag{A6}$$

where $\Pi \equiv VV^\dagger$. From the monotonicity of quantum relative entropy with respect to quantum channels [28, 29], we find that

$$D(\omega_{ZZ'AB}\|I_Z \otimes \omega_{Z'AB}) \geqslant D(\mathcal{P}_{ZZ'A}(\omega_{ZZ'AB})\|\mathcal{P}_{ZZ'A}(I_Z \otimes \omega_{Z'AB})). \tag{A7}$$

Consider that $\mathcal{P}_{ZZ'A}(\omega_{ZZ'AB}) = \omega_{ZZ'AB}$. Due to the fact that

$$(I-\Pi)\omega_{ZZ'AB}(I-\Pi) = 0, \tag{A8}$$

and from the direct sum property of the quantum relative entropy (see, e.g., [33]), we have that

$$D(\mathcal{P}_{ZZ'A}(\omega_{ZZ'AB})\|\mathcal{P}_{ZZ'A}(I_Z \otimes \omega_{Z'AB})) = D(\omega_{ZZ'AB}\|\Pi(I_Z \otimes \omega_{Z'AB})\Pi). \tag{A9}$$

Consider that

$$\Pi(I_Z \otimes \omega_{Z'AB})\Pi = VV^\dagger(I_Z \otimes \omega_{Z'AB})VV^\dagger = V\left(\sum_z Q_A^z \rho_{AB} Q_A^z\right)V^\dagger. \tag{A10}$$

This, combined with $\omega_{ZZ'AB} = V\rho_{AB}V^\dagger$, then implies that

$$D(\omega_{ZZ'AB}\|\Pi(I_Z \otimes \omega_{Z'AB})\Pi) = D\left(V\rho_{AB}V^\dagger\|V\left(\sum_z Q_A^z\rho_{AB}Q_A^z\right)V^\dagger\right) \tag{A11}$$

$$= D\left(\rho_{AB}\|\sum_z Q_A^z\rho_{AB}Q_A^z\right), \tag{A12}$$

where the last equality follows from the invariance of quantum relative entropy with respect to isometries. Now consider the following quantum channel:

$$\mathcal{M}_{A\to X} \equiv \mathrm{Tr}_{X'A} \circ \mathcal{U}_{A\to XX'A}, \tag{A13}$$

where $\mathcal{U}_{A\to XX'A}(\cdot) \equiv U(\cdot)U^\dagger$. Consider that $\mathcal{M}_{A\to X}(\rho_{AB}) = \sigma_{XB}$. Also, we can calculate

$$\mathcal{M}_{A\to X}\left(\sum_z Q_A^z\rho_{AB}Q_A^z\right) \tag{A14}$$

as follows:

$$(\mathrm{Tr}_{X'A} \circ \mathcal{U}_{A\to XX'A})\left(\sum_z Q_A^z\rho_{AB}Q_A^z\right) = \theta_{XB}. \tag{A15}$$

From [24], we have the following inequality holding for a density operator ρ, a positive semi-definite operator σ, and a quantum channel $\mathcal{N}$:

$$D(\rho\|\sigma) - D(\mathcal{N}(\rho)\|\mathcal{N}(\sigma)) \geqslant -\log F(\rho, \mathcal{R}(\mathcal{N}(\rho))), \tag{A16}$$

where $\mathrm{supp}(\rho) \subseteq \mathrm{supp}(\sigma)$ and $\mathcal{R}$ is a recovery channel with the property that $\mathcal{R}(\mathcal{N}(\sigma)) = \sigma$. Specifically, $\mathcal{R}$ is what is known as a variant of the Petz recovery channel, having the form

$$\mathcal{R}(\cdot) \equiv \int \mathrm{d}t\; p(t)\sigma^{-\mathrm{i}t/2}\mathcal{R}_{\sigma,\mathcal{N}}(\mathcal{N}(\sigma)^{\mathrm{i}t/2}(\cdot)\mathcal{N}(\sigma)^{-\mathrm{i}t/2})\sigma^{\mathrm{i}t/2}$$
$$\text{with} \quad p(t) \equiv \frac{\pi}{2}(\cosh(\pi t) + 1)^{-1}, \tag{A17}$$

where $\mathcal{R}_{\sigma,\mathcal{N}}$ is the Petz recovery channel [42–44] defined as

$$\mathcal{R}_{\sigma,\mathcal{N}}(\cdot) \equiv \sigma^{1/2}\mathcal{N}^{\dagger}(\mathcal{N}(\sigma)^{-1/2}(\cdot)\mathcal{N}(\sigma)^{-1/2})\sigma^{1/2}, \tag{A18}$$

with $\mathcal{N}^{\dagger}$ the adjoint of $\mathcal{N}$ (with respect to the Hilbert–Schmidt inner product). Applying this to our case, we find that

$$D\left(\rho_{AB}\|\sum_z Q_A^z \rho_{AB} Q_A^z\right) \geqslant D\left(\mathcal{M}_{A\to X}(\rho_{AB})\|\mathcal{M}_{A\to X}\left(\sum_z Q_A^z \rho_{AB} Q_A^z\right)\right)$$
$$- \log F(\rho_{AB}, \mathcal{R}_{XB\to AB}(\mathcal{M}_{A\to X}(\rho_{AB}))), \tag{A19}$$

where the recovery channel is such that

$$\mathcal{R}_{XB\to AB}\left(\mathcal{M}_{A\to X}\left(\sum_z Q_A^z \rho_{AB} Q_A^z\right)\right) = \sum_z Q_A^z \rho_{AB} Q_A^z. \tag{A20}$$

Consider from our development above that

$$D\left(\mathcal{M}_{A\to X}(\rho_{AB})\|\mathcal{M}_{A\to X}\left(\sum_z Q_A^z \rho_{AB} Q_A^z\right)\right) = D(\sigma_{XB}\|\theta_{XB}) \tag{A21}$$
$$\geqslant D(\sigma_{XB}\|I_X \otimes \sigma_B) - \log c, \tag{A22}$$

where we have used $\sigma \leqslant \sigma' \Rightarrow D(\rho\|\sigma') \leqslant D(\rho\|\sigma)$ (see, e.g., [33]), applied to $Q_A^z P_A^x Q_A^z = |Q_A^z P_A^x|^2 \leqslant c \cdot I_A$, with c defined in (5). Putting everything together, we conclude that

$$D(\omega_{ZZ'AB}\|I_Z \otimes \omega_{Z'AB}) \geqslant D(\sigma_{XB}\|I_X \otimes \sigma_B) - \log c - \log F(\rho_{AB}, \mathcal{R}_{XB\to AB}(\sigma_{XB})), \tag{A23}$$

which, after a rewriting, is equivalent to (7) coupled with the constraint in (A20).

The inequality in (8) follows from (7) by letting $|\psi\rangle_{ABE}$ be a purification of ρ_{AB} and observing that

$$H(Z|E)_{\omega} - H(Z|B)_{\omega} = -H(A|B)_{\rho}, \tag{A24}$$

whenever ρ_{ABE} is a pure state and $Q_A^z = |z\rangle\langle z|_A$ for some orthonormal basis $\{|z\rangle_A\}_z$.

Appendix B. Explicit form of recovery map

Here we establish the explicit form given in (10) for the recovery map, in the case that $\{Q_A^z = |z\rangle\langle z|_A\}$ for some orthonormal basis $\{|z\rangle_A\}_z$. The main idea is to determine what $\mathcal{R}_{XB\to AB}$ in (A19) should be by inspecting (A16) and (A17). For our setup, we are considering a bipartite state ρ_{AB}, a set $\{Q_A^z\}$ of measurement operators, and the measurement channel

$$\mathcal{M}_{A\to X}(\zeta_A) \equiv \sum_x \mathrm{Tr}\{P_A^x \zeta_A\}|x\rangle\langle x|_X, \tag{B1}$$

where $\{P_A^x\}_x$ is a set of projective measurement operators. The entropy inequality in (A19) reduces to

$$D\left(\rho_{AB}\|\sum_z |z\rangle\langle z|_A \otimes \omega_B^z\right) - D\left(\mathcal{M}_{A\to X}(\rho_{AB})\|\sum_x |x\rangle\langle x|_X \otimes \theta_B^x\right)$$
$$\geqslant -\log F(\rho_{AB}, \mathcal{R}_{XB\to AB}(\mathcal{M}_{A\to X}(\rho_{AB}))), \tag{B2}$$

where

$$\omega_B^z \equiv (\langle z|_A \otimes I_B)\rho_{AB}(|z\rangle_A \otimes I_B), \qquad \theta_B^x \equiv \sum_z \langle z|_A P_A^x |z\rangle_A \omega_B^z. \tag{B3}$$

Observe that

$$\sum_x |x\rangle\langle x|_X \otimes \theta_B^x = \mathcal{M}_{A\to X}\left(\sum_z |z\rangle\langle z|_A \otimes \omega_B^z\right). \tag{B4}$$

Writing the measurement channel as

$$\mathcal{M}_{A\to X}(\zeta_A) \equiv \sum_x \mathrm{Tr}\{P_A^x \zeta_A P_A^x\} |x\rangle\langle x|_X = \sum_{x,j} \langle j|_A P_A^x \zeta_A P_A^x |j\rangle_A |x\rangle\langle x|_X \tag{B5}$$

$$= \sum_{x,j} |x\rangle_X \langle j|_A P_A^x \zeta_A P_A^x |j\rangle_A \langle x|_X, \tag{B6}$$

we can see that a set of Kraus operators for it is $\{|x\rangle_X \langle j|_A P_A^x\}_{x,j}$. So its adjoint is as follows:

$$(\mathcal{M}_{A\to X})^\dagger(\kappa_X) = \sum_{x,j} P_A^x |j\rangle_A \langle x|_X \kappa_X |x\rangle_X \langle j|_A P_A^x = \sum_{x,j} \langle x|_X \kappa_X |x\rangle_X P_A^x |j\rangle_A \langle j|_A P_A^x \tag{B7}$$

$$= \sum_x \langle x|_X \kappa_X |x\rangle_X P_A^x. \tag{B8}$$

So by inspecting (A16) and (A17), we see that the recovery map has the following form:

$$\begin{aligned}
&\mathcal{R}_{XB\to AB}(\xi_{XB}) \\
&= \int \mathrm{d}t\ p(t) \left(\sum_z |z\rangle\langle z|_A \otimes \omega_B^z\right)^{\frac{1-it}{2}} \sum_x P_A^x (\langle x|_X \otimes I_B) \left(\sum_{x'} |x'\rangle\langle x'|_X \otimes \theta_B^{x'}\right)^{\frac{-1+it}{2}} (\xi_{XB}) \\
&\quad \times \left(\sum_{x''} |x''\rangle\langle x''|_X \otimes \theta_B^{x''}\right)^{\frac{-1-it}{2}} (|x\rangle_X \otimes I_B) \left(\sum_{z'} |z'\rangle\langle z'|_A \otimes \omega_B^{z'}\right)^{\frac{1+it}{2}},
\end{aligned} \tag{B9}$$

$$\begin{aligned}
&= \int \mathrm{d}t\ p(t) \left(\sum_z |z\rangle\langle z|_A \otimes (\omega_B^z)^{\frac{1-it}{2}}\right) \sum_x P_A^x (\langle x|_X \otimes I_B) \\
&\quad \times \left[\left(\sum_{x'} |x'\rangle\langle x'|_X \otimes (\theta_B^{x'})^{\frac{-1+it}{2}}\right) (\xi_{XB}) \left(\sum_{x''} |x''\rangle\langle x''|_X \otimes (\theta_B^{x''})^{\frac{-1-it}{2}}\right)\right] \\
&\quad \times (|x\rangle_X \otimes I_B) \left(\sum_{z'} |z'\rangle\langle z'|_A \otimes (\omega_B^{z'})^{\frac{1+it}{2}}\right),
\end{aligned} \tag{B10}$$

$$\begin{aligned}
&= \int \mathrm{d}t\ p(t) \left(\sum_z |z\rangle\langle z|_A \otimes (\omega_B^z)^{\frac{1-it}{2}}\right) \sum_{x,x',x''} P_A^x \langle x|_X |x'\rangle\langle x'|_X \otimes (\theta_B^{x'})^{\frac{-1+it}{2}} (\xi_{XB}) \\
&\quad \times |x''\rangle\langle x''|_X |x\rangle_X \otimes (\theta_B^{x''})^{\frac{-1-it}{2}} \left(\sum_{z'} |z'\rangle\langle z'|_A \otimes (\omega_B^{z'})^{\frac{1+it}{2}}\right),
\end{aligned} \tag{B11}$$

$$\begin{aligned}
&= \int \mathrm{d}t\ p(t) \left(\sum_z |z\rangle\langle z|_A \otimes (\omega_B^z)^{\frac{1-it}{2}}\right) \sum_x P_A^x \langle x|_X \otimes (\theta_B^x)^{\frac{-1+it}{2}} (\xi_{XB}) |x\rangle_X \otimes (\theta_B^x)^{\frac{-1-it}{2}} \\
&\quad \times \left(\sum_{z'} |z'\rangle\langle z'|_A \otimes (\omega_B^{z'})^{\frac{1+it}{2}}\right),
\end{aligned} \tag{B12}$$

$$= \int \mathrm{d}t\ p(t) \sum_{z,x,z'} |z\rangle\langle z|_A P_A^x |z'\rangle\langle z'|_A \otimes (\omega_B^z)^{\frac{1-it}{2}} (\theta_B^x)^{\frac{-1+it}{2}} \mathrm{Tr}_X\{|x\rangle\langle x|_X (\xi_{XB})\} (\theta_B^x)^{\frac{-1-it}{2}} (\omega_B^{z'})^{\frac{1+it}{2}}. \tag{B13}$$

We can thus abbreviate its action as

$$\mathcal{R}_{XB\to AB}(\xi_{XB}) = \sum_{z,x,z'} |z\rangle\langle z|_A P_A^x |z'\rangle\langle z'|_A \otimes \mathcal{R}_{XB\to B}^{x,z,z'}(\xi_{XB}), \tag{B14}$$

where

$$\mathcal{R}_{XB\to B}^{x,z,z'}(\xi_{XB}) \equiv \int \mathrm{d}t\ p(t) (\omega_B^z)^{\frac{1-it}{2}} (\theta_B^x)^{\frac{-1+it}{2}} \mathrm{Tr}_X\{|x\rangle\langle x|_X (\xi_{XB})\} (\theta_B^x)^{\frac{-1-it}{2}} (\omega_B^{z'})^{\frac{1+it}{2}}. \tag{B15}$$

(Note that $\mathcal{R}_{XB\to B}^{x,z,z'}$ is not a channel.) So then the action on the classical-quantum state σ_{XB}, defined as

$$\sigma_{XB} \equiv \sum_x |x\rangle\langle x|_X \otimes \sigma_B^x, \tag{B16}$$

with $\sigma_B^x \equiv \mathrm{Tr}_A\{P_A^x \rho_{AB}\}$, is as follows:

$$\mathcal{R}_{XB\to AB}(\sigma_{XB}) = \sum_{z,x,z'} |z\rangle\langle z|_A P_A^x |z'\rangle\langle z'|_A \otimes \int \mathrm{d}t\ p(t) (\omega_B^z)^{\frac{1-it}{2}} (\theta_B^x)^{\frac{-1+it}{2}} \sigma_B^x (\theta_B^x)^{\frac{-1-it}{2}} (\omega_B^{z'})^{\frac{1+it}{2}}. \tag{B17}$$

References

[1] Heisenberg W 1927 Über den anschaulichen inhalt der quantentheoretischen kinematik und mechanik *Z. Phys.* **43** 172–98
[2] Berta M, Christandl M, Colbeck R, Renes J M and Renner R 2010 The uncertainty principle in the presence of quantum memory *Nat. Phys.* **6** 659–62
[3] Robertson H P 1929 The uncertainty principle *Phys. Rev.* **34** 163
[4] Hirschman I I 1957 A note on entropy *Am. J. Math.* **79** 152–6
[5] Bialynicki-Birula I and Mycielski J 1975 Uncertainty relations for information entropy in wave mechanics *Commun. Math. Phys.* **44** 129–32
[6] Beckner W 1975 Inequalities in Fourier analysis *Ann. Math.* **102** 159
[7] Deutsch D 1983 Uncertainty in quantum measurements *Phys. Rev. Lett.* **50** 631–3
[8] Kraus K 1987 Complementary observables and uncertainty relations *Phys. Rev.* D **35** 3070–5
[9] Maassen H and Uffink J B M 1988 Generalized entropic uncertainty relations *Phys. Rev. Lett.* **60** 1103–6
[10] Krishna M and Parthasarathy K R 2002 An entropic uncertainty principle for quantum measurements *Sankhya: Indian J. Stat. Ser.* A **64** 842–51
[11] Christandl M and Winter A 2005 Uncertainty, monogamy, and locking of quantum correlations *IEEE Trans. Inf. Theory* **51** 3159–65
[12] Renes J M and Boileau J-C 2009 Conjectured strong complementary information tradeoff *Phys. Rev. Lett.* **103** 020402
[13] Coles P J, Berta M, Tomamichel M and Wehner S 2015 Entropic uncertainty relations and their applications arXiv:1511.04857
[14] Terhal B M 2004 Is entanglement monogamous? *IBM J. Res. Dev.* **48** 71–8
[15] Almheiri A, Marold D, Polchinski J and Sully J 2013 Black holes: complementarity or firewalls? *J. High Energy Phys.* JHEP02(2013)062
[16] Naimark M A 1940 Spectral functions of a symmetric operator *Izv. Acad. nauk SSSR Ser. Mat.* **4** 277–318
[17] Tomamichel M, Fehr S, Kaniewski J and Wehner S 2013 A monogamy-of-entanglement game with applications to device-independent quantum cryptography *New J. Phys.* **15** 103002
[18] Tomamichel M and Renner R 2011 Uncertainty relation for smooth entropies *Phys. Rev. Lett.* **106** 110506
[19] Tomamichel M, Ci Wen Lim C, Gisin N and Renner R 2012 Tight finite-key analysis for quantum cryptography *Nat. Commun.* **3** 634
[20] Tomamichel M and Leverrier A 2015 A rigorous and complete proof of finite key security of quantum key distribution arXiv:1506.08458
[21] Coles P J, Yu L and Zwolak M 2011 Relative entropy derivation of the uncertainty principle with quantum side information arXiv:1105.4865
[22] Frank R L and Lieb E H 2013 Extended quantum conditional entropy and quantum uncertainty inequalities *Commun. Math. Phys.* **323** 487–95
[23] Furrer F, Berta M, Tomamichel M, Scholz V B and Christandl M 2014 Position-momentum uncertainty relations in the presence of quantum memory *J. Math. Phys.* **55** 122205
[24] Junge M, Renner R, Sutter D, Wilde M M and Winter A 2015 Universal recovery from a decrease of quantum relative entropy arXiv:1509.07127
[25] Wilde M M 2015 Recoverability in quantum information theory *Proc. R. Soc.* A **471** 20150338
[26] Sutter D, Tomamichel M and Harrow A W 2016 Strengthened monotonicity of relative entropy via pinched Petz recovery map *IEEE Trans. Inf. Theory* **62** 2907–13
[27] Sutter D, Berta M and Tomamichel M 2016 Multivariate trace inequalities arXiv:1604.03023
[28] Lindblad G 1975 Completely positive maps and entropy inequalities *Commun. Math. Phys.* **40** 147–51
[29] Uhlmann A 1977 Relative entropy and the Wigner–Yanase–Dyson–Lieb concavity in an interpolation theory *Commun. Math. Phys.* **54** 21–32
[30] Wilde M M 2013 *Quantum Information Theory* (Cambridge: Cambridge University Press)
[31] Sagawa T 2012 Second law-like inequalities with quantum relative entropy: an introduction *Lectures on Quantum Computing, Thermodynamics and Statistical Physics* (Singapore: World Scientific) p 127 arXiv:1202.0983
[32] Uhlmann A 1976 The 'transition probability' in the state space of *a* *-algebra *Rep. Math. Phys.* **9** 273–9
[33] Coles P J, Colbeck R, Yu L and Zwolak M 2012 Uncertainty relations from simple entropic properties *Phys. Rev. Lett.* **108** 210405
[34] IBM, The quantum experience, http://research.ibm.com/quantum/
[35] Alsina D and Latorre J 2016 Experimental test of Mermin inequalities on a 5-qubit quantum computer arXiv:1605.04220
[36] Devitt S J 2016 Performing quantum computing experiments in the cloud arXiv:1605.05709
[37] Rundle R P, Tilma T, Samson J H and Everitt M J 2016 Quantum state reconstruction made easy: a direct method for tomography arXiv:1605.08922
[38] Nielsen M A and Chuang I L 2000 *Quantum Computation and Quantum Information* (Cambridge: Cambridge University Press)
[39] Dupuis F, Fawzi O and Wehner S 2015 Entanglement sampling and its applications *IEEE Trans. Inf. Theory* **61** 1093–112
[40] Forrest Stinespring W 1955 Positive functions on C^*-algebras *Proc. Am. Math. Soc.* **6** 211–6
[41] Umegaki H 1962 Conditional expectations in an operator algebra IV (entropy and information) *Kodai Math. Semin. Rep.* **14** 59–85
[42] Petz D 1986 Sufficient subalgebras and the relative entropy of states of a von Neumann algebra *Commun. Math. Phys.* **105** 123–31
[43] Petz D 1988 Sufficiency of channels over von Neumann algebras *Q. J. Math.* **39** 97–108
[44] Hayden P, Jozsa R, Petz D and Winter A 2004 Structure of states which satisfy strong subadditivity of quantum entropy with equality *Commun. Math. Phys.* **246** 359–74